

# COMSOL Modelling and Simulation of PEM Fuel Cell's Flow Channels

Eric Robalinho<sup>1</sup>, Edgar F Cunha<sup>1</sup>, Alexandre B Andrade<sup>1</sup>,  
Martha L M Bejarano<sup>1</sup>, Marcelo Linardi<sup>1</sup>, Efraim Cekinski<sup>2</sup>

<sup>1</sup> Instituto de Pesquisas Energéticas e Nucleares (IPEN / CNEN - SP)  
Av. Professor Lineu Prestes 2242  
05508-000 São Paulo, SP  
eric@ipen.br  
efcunha@ipen.br  
abodart@ipen.br  
mmora@ipen.br  
mlinardi@ipen.br

<sup>2</sup> Instituto de Pesquisas Tecnológicas (IPT - SP)  
Av. Prof. Almeida Prado, 532  
05508-901 São Paulo, SP  
cekinski@ipt.br

**Abstract:** Fuel cells are one of the most important devices to obtain electrical energy from hydrogen. The Computational Fluid Dynamic (CFD) is a very useful tool to explore the connection between the transport of reactants and products within the fuel cell and overall cell performance. CFD simulates hydrogen and oxygen gases flow channels to reduce the costs of bipolar plates' production through optimization of the mass transport. In this work, two configurations of gas flow channels were studied by simulation with COMSOL software and a preliminary experimental test to verify the model applied in these configurations was performed. Two single Proton Exchange Membrane Fuel Cells – PEMFC – with 144 cm<sup>2</sup> of active area were manufactured. The first one (1) was a commercial graphite plate supplied by ELECTROCELL. The other one (2) was projected and constructed at IPEN. The serpentine flow field was chosen. The dimensions of flow field of prototype 1 were: 2 mm width and 2 mm depth channels and 2 mm ribs. In this case each part of the serpentine flow field was composed by 6 channels and 5 ribs. The dimensions of flow field of prototype 2 were: 1.5 mm width and 1.5 mm depth channels and 0.5 mm ribs. For this prototype, each part of serpentine flow field was composed by 12 channels and 11 ribs. A mesh study was performed on the 3D models to determine the minimum number of elements required to

accurately solve the equations over the solution domain. Process simulations of diffusion in porous media and conduction/convection were studied. Once all of the global iterations had been completed, the experimental data were compared with modelling results. The graphite plate B exhibited better performance than the A one, that was validated by numeric methods. Such behavior was attributed to the higher channel area in contact with gas diffusion electrode which provides higher active area available for the gas reaction. Besides the area, higher gas velocities in flow fields decrease the gas stagnation points along the channels.

**Keywords:** Numerical model, CFD simulation, PEMFC, hydrogen technology.

## 1. Introduction

Fuel cells and hydrogen technology represent the most promising alternative pathway for automotive and stationary applications. The PEMFC offers low to zero emission for subWatt to MWatt power generation, meaning applications in transportation, industries and portable supplies units [1,2]. In this paper the role of computational tools was studied in order to verify some experimental results and demonstrate the better performance of PEMFC constructed from optimizations techniques.

The PEMFC is an electrochemical device and consists of two principal parts: (i) an electrolyte between two electrodes, an anode and a cathode with two diffusion layers, called Membrane Electrode Assembly (MEA) and (ii) gas flow field plates, called bipolar plates, in case of the stack. The plates have many functions in a fuel cell [3]: distribute reactant gases (hydrogen and air or oxygen) uniformly, collect and conduct electrical current and remove heat and water from the electrodes. The bipolar plates make the cell robust and give a rigid structure to support the impacts of portable and automotive applications. The cost of the bipolar plates corresponds up to 45% of the total cost and about 80% of the total weight in a stack fuel cell [4,5].

The search for reliable computational models is a challenge because it involves several transport phenomena: multi-component, multi-phase and multi-dimensional flow processes, electrochemical reactions, convective heat and mass transport in flow channels, diffusion of reactants through porous electrodes, transport of water through the membrane and transport of electrons through solid matrix.

The Computational Fluid Dynamic (CFD) is a very useful tool to simulate hydrogen and oxygen gases flow channels configurations, reducing the costs of bipolar plates' production and optimizing mass transport [6-8].

## 2. Methodology

Two single cells of 144 cm<sup>2</sup> of active area were manufactured, called prototype 1 and prototype 2. The serpentine flow field was chosen for channel geometry. The configuration of flow field in the prototype 1 was: 2 mm width and 2 mm depth channels and 2 mm ribs. In this case each part of the serpentine flow field was composed by 6 channels and 5 ribs. The flow field of prototype 2 was: 1.5 mm width and 1.5 mm depth channels and 0.5 mm ribs. For this prototype, each part of serpentine flow field was composed by 12 channels and 11 ribs. In Figure 1 (a) and (b) the bipolar plates of prototype 1 and prototype 2 were showed, respectively. For these flow field configurations, the prototype 2 has 50 % more channel area than prototype 1 (0.110 m<sup>2</sup> and 0.073 m<sup>2</sup> respectively).

The best-known membrane electrolyte material for PEM fuel cell is Nafion<sup>TM</sup> membrane by Dupont, which has high proton conductivity. Besides the membrane, the MEA is composed by two electrodes as catalytic layers, using platinum supported in carbon black as electro catalysts; and two gas diffusion layers (GDL) like carbon paper or carbon cloth. Fuel cell polarization measurements were carried out galvanostatically with the single cell at 70 °C, using oxygen and hydrogen with saturated water vapor (Millipore quality – Elix 3 model) at 85 °C, at atmospheric pressure and hydrogen volumetric flux 8.33 10<sup>-6</sup> m<sup>3</sup> s<sup>-1</sup>.



**Figure 1:** Flow field channels from prototype 1 (a) and prototype 2 (b).

### 3. Numerical Models

The efforts of this work were concentrated in two goals. The first part was the analysis of four partial geometries consisting of the inlet and two channels with the porous media. Then, in the second place, two graphite plates were simulated to investigate the hydrogen flow, pressure drops and temperature distribution. Implementations of the modeling allowed the optimization the design of the plates and better understanding the fuel cell dynamics.

The Nonlinear solver for stationary analysis was set automatically by COMSOL, and the Spooles direct solver was selected for linear conditions [9]. The Spooles uses the multifrontal method and direct LU factorization of the sparse matrix  $A$  when solves systems of the form  $Ax=b$ . There are several solver methods available at COMSOL Multiphysics, including the iterative ones that are the natural choice for problems with many degrees of freedom. However the iterative solvers are less stable than direct solvers and they do not always converge.

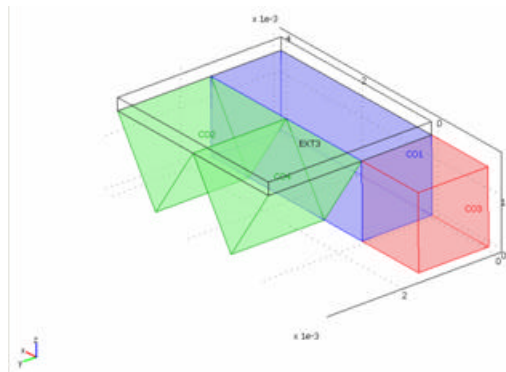


**Figure 2:** Partial triangular geometry.

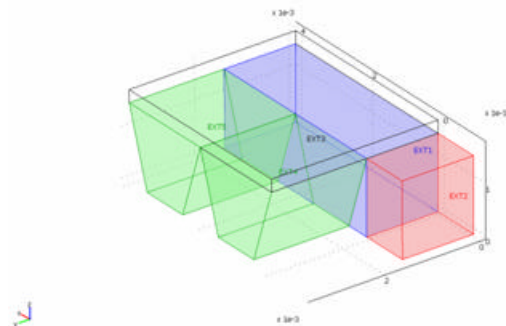


**Figure 3:** Partial trapezoidal geometry.

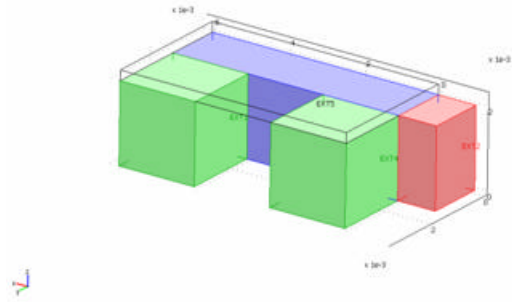


**Figure 4:** Partial 2 mm square geometry.

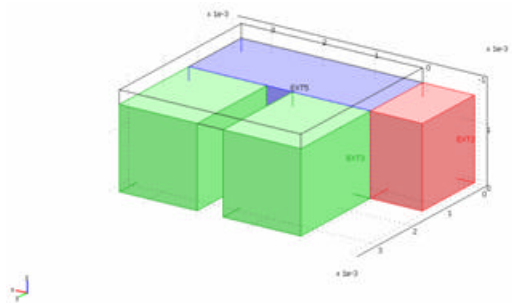


**Figure 5:** Partial 1.5 mm square geometry.

In Figures 2-5 the channels geometries are showed. The red region represents the gas inlet, the blue one is the distribution place and the green is the initial part of two channels. The area above the channels (0.25 mm thickness transparent rectangle) is the GDL. The triangular and the trapezoidal geometries have 1.5 mm depth. In the Figures 2-5 the x, y and z axis are showed.

In the Table 1 the different meshes and corresponding solutions time were compared. The convergence in these cases was obtained in 3 to 7 iterations and the relative tolerance at nonlinear solver was set on  $1.0E-6$ . The refinement method was set on longest, with the best quality option. The mesh in each simulation is defined by the Number of Degrees of Freedom (NOF'S), the Number of Elements (NE) and the Minimum Element Quality (MEQ). As one can see at Table 1, the refinement of the mesh means much more solution time and availability of memory.

The flow distribution is described by two equations: Navier-Stokes (Eq.1.) and continuity (Eq.2.),

$$\mathbf{r} \frac{\partial \mathbf{u}}{\partial t} - \nabla \cdot \mathbf{h} (\nabla \mathbf{u} + (\nabla \mathbf{u})^T) + \mathbf{r} (\mathbf{u} \cdot \nabla) \mathbf{u} + \nabla p = 0 \quad (1)$$

$$\nabla \cdot \mathbf{u} = 0 \quad (2)$$

where  $\mathbf{r}$  denotes the density [ $\text{kg m}^{-3}$ ],  $\mathbf{u}$  the velocity vector [ $\text{m s}^{-1}$ ],  $\mathbf{h}$  the viscosity [ $\text{N s m}^{-2}$ ], and  $\mathbf{p}$  the pressure [Pa]. The density and viscosity of the modeled gases were calculated in function of the pressure and temperature using models offered for the CFD software.

The model uses normal/pressure boundary conditions for inlet and convective flux for outlet. The condition for porosity (porous media) was found in Navier-Stokes module in COMSOL version 3.3, which was set on  $1.0\text{E-}12 \text{ m}^2$  for permeability of GDL.

The results in Table 1 and the pos-processing Figures and Graphics were obtained at Intel 5320 Quad Core XEON Workstation with 4 GB RAM.

**Table 1:** Different meshes and corresponding NOF'S, NE, MEQ and SOLUTION TIME.

	MESH	NOF'S	NE	MEQ	SOLUTION TIME (s)
TRIANGULAR	Coarser	7351	957	0.2829	9.1
	Coarse	10808	1464	0.2990	14.6
	Normal	16111	2298	0.2500	27.4
	Fine	30187	4498	0.3756	98.7
	Finer	83234	13081	0.3558	1158.3
TRAPEZOIDAL	Coarser	8305	996	0.3339	12.7
	Coarse	13399	1689	0.3566	29.1
	Normal	21845	3064	0.3656	113.6
	Fine	45315	6560	0.2509	551.8
	Finer	119717	18594	0.3401	5239.1
SQUARE (2mm)	Coarser	6729	769	0.3080	9.2
	Coarse	10425	1273	0.2944	17.7
	Normal	19148	2563	0.3498	56.2
	Fine	29260	4144	0.3696	149.8
	Finer	83845	12718	0.3422	1891.2
SQUARE (1.5mm)	Coarser	7496	937	0.3230	12.7
	Coarse	14962	1867	0.2823	42.3
	Normal	31808	4509	0.3195	241.5
	Fine	56461	8369	0.3868	908.5
	Finer	158145	24959	0.2715	17592.2

#### 4. Results & Discussions

Pressure lines graphics were plotted for each profile studied. For one predetermined channel length,  $y = 3.50\text{mm}$ , six pressure lines were plotted at the GDL interior and one at the channel outlet (0.05mm from the upper surface of the channel), in order to evaluate the pressure gradient there. The pressure gradient behavior of the studied models provides homogeneity of the

reactants gas flux data through diffusion layer. A homogeneous pressure gradient means higher gas availability for the fuel cell reactions.

According to the graphics shown, a huge stagnation region (dead zone) is noticed at the top of rib between the 2mm square profile channels. In Figure 8 this effect is noticed from the inexistence of a high pressure gradient at  $2.50\text{mm} < x < 3.50\text{mm}$  range (every pressure lines were close to zero).

The 1.5 square profile presents stagnation, but it is local surrounding  $x=1.75\text{mm}$  (Figure 9).

The trapezoidal and triangular profile channels presented similar responses about pressure gradient throughout the geometry, with no stagnation zones.

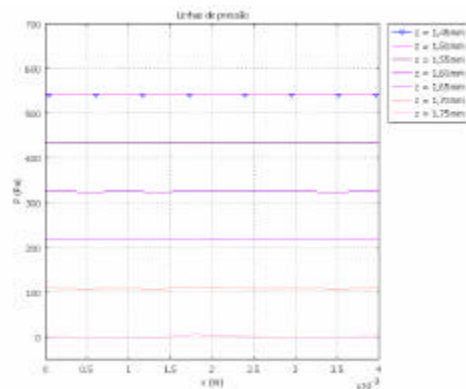


Figure 6: Pressure lines of triangular profile.

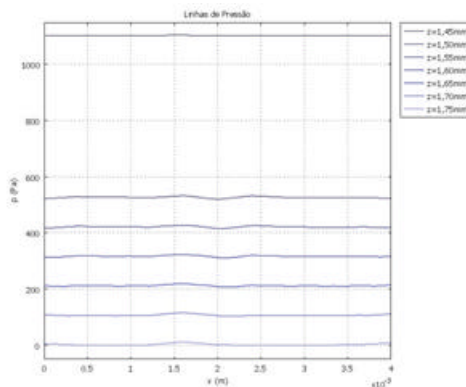


Figure 7: Pressure lines of trapezoidal profile.

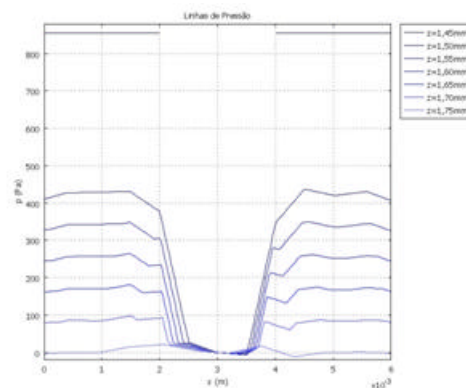


Figure 8: Pressure lines of 2mm square profile.

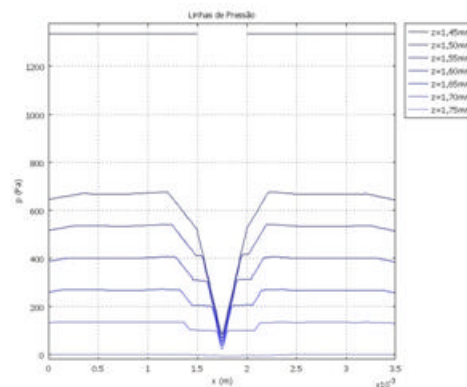


Figure 9: Pressure lines of 1.5mm square profile.

In the Figures 10-13 the z-velocity slice profiles for all channels configurations are showed.

At velocity slice graphic (Figure 12) of 2mm square profile, there is a remarkable region of low velocity in z, confirming the obtained results by pressure lines.

Although both triangular and trapezoidal profiles presented pressure gradient ( $p \sim 0.55 \text{ kPa}$  at GDL) below of the 1.5mm square profile ( $p \sim 0.65 \text{ kPa}$  at GDL), the z-direction velocity profile stood around  $0.2 \text{ m.s}^{-1}$  throughout x-axis; the square profiles, instead, presented areas or spots of large velocity decreasing (hitting  $0.1 \text{ m.s}^{-1}$  at diffusion layer outlet,  $z=2.25\text{mm}$  at 2mm square profile and  $z=1.75\text{mm}$  at 1.5 square profile).

In order to check the studied models correspondence within fuel cell experiments, both square profiles (graphite plates) were used.

The polarization curve measures the fuel cell performance in terms of potential, under different values of current. The value of  $0.6\text{V}$  (work potential), is set to compare two different fuel cells performance.

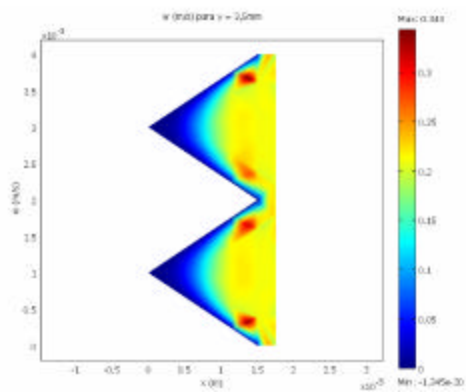


**Figure 10:** z-velocity slice of triangular profile.

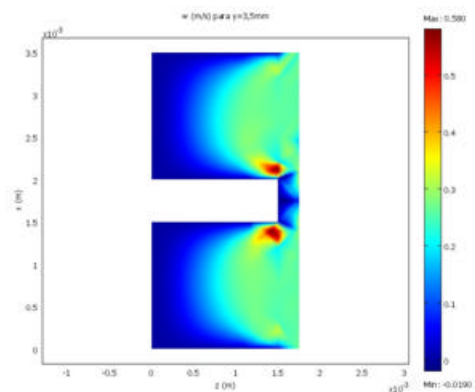


**Figure 13:** z-velocity slice of 1.5mm square profile.

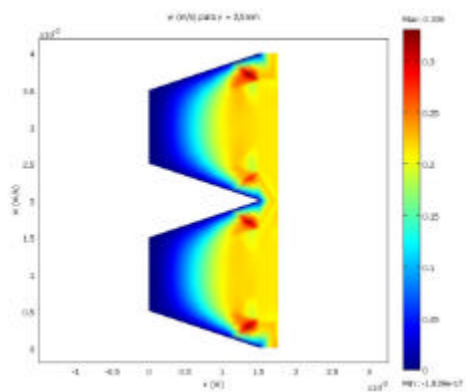


**Figure 11:** z-velocity slice of trapezoidal profile.

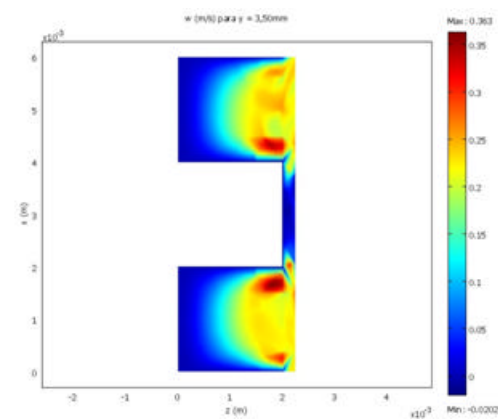


**Figure 12:** z-velocity slice of 2mm square profile.

In Figure 14 the polarization curves of the both prototypes were presented. The values for work operation were:  $166.7\text{mA cm}^{-2}$  and  $470.6\text{mA cm}^{-2}$ , for the prototype 1 and 2, respectively.

The graphite plate in prototype 2 had better performance than in the prototype 1, which was validated by numeric methods. Such behavior was attributed to the higher channel area in contact with gas diffusion electrode which provides higher active area available for the gas reaction. Besides the area, higher gas velocities in flow fields decrease the gas stagnation points along the channels.

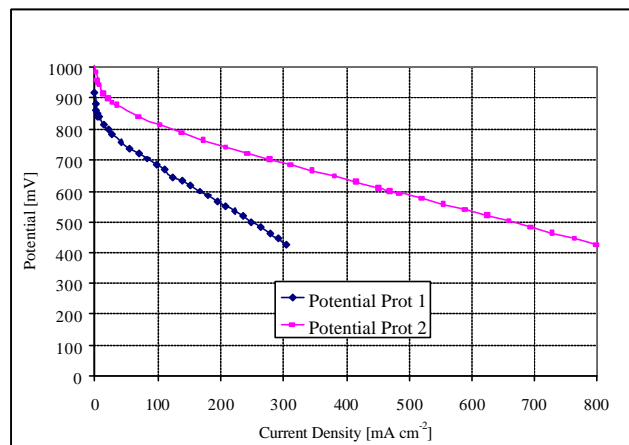


**Figure 14:** Polarization curves of prototype 1 and prototype 2.

## 5. Conclusions

The CFD techniques help the fuel cell's researchers to explore the connection between the transport of reactants and products and overall cell performance. CFD simulates hydrogen gas flow channels to reduce the costs of bipolar plates' production through optimization of the mass transport. New geometries are proposed and tested at laboratory scale.

Several models' simulations of diffusion in porous media and conduction/convection processes were studied. Then, the experimental data were used to visualize the differences in performance between PEMFC 1 and 2. The graphite plate in prototype 2 exhibited better performance than in prototype 1, which was validated by numeric methods. Such behavior was attributed to the higher channel area in contact with gas diffusion electrode which provides higher active area available for the gas reaction. Besides the area, higher gas velocities in flow fields decrease the gas stagnation points along the channels.

## 6. Acknowledgements

This work was supported by IPEN/CNEN-SP at PROCEL laboratories.

## 7. References

1. N. Djilali, Computational modeling of polymer electrolyte membrane (PEM) fuel cells: Challenges and opportunities, *Energy* (2006), doi:10.1016/j.energy.2006.08.007.
2. E.F. Cunha, A.B. Andrade, E. Robalinho, M.L.M. Bejarano, E. Cekinski, M. Linardi, Modeling and simulation of PEM fuel cell's flow channels using CFD techniques, *International Nuclear Atlantic Conference – INAC*, 2007.
3. E. Middelmann, W. Kout, B. Vogelaar, J. Lensen, E. de Waal, Bipolar plates for PEM fuel cells, *Journal of Power Sources*, **Volume 118**, pp.44-46 (2003).
4. A. Kummar, R.G. Reddy, Materials and design development for bipolar/end plates in fuel cell, *Journal of Power Sources*, **Volume 129**, pp.62-67 (2004).
5. W. Quian, D. P. Wilkson, J. Shen, H. Wang, J. Zhang, Architecture for portable direct liquid fuel cells, *Journal of Power Sources*, **Volume 154**, pp.202-213 (2006).
6. P.T. Nguyen, T. Berning, N. Djilali, Computational model of PEM fuel cell with serpentine gas flow channels, *Journal of Power Sources*, **Volume 130**, pp.149-157 (2004).
7. S. Karvonen, T. Rottinen, J. Saarinen, O. Himanen, Modeling of flow field in polymer electrolyte membrane fuel cell, *Journal of Power Sources*, **Volume 161**, pp.876-884 (2006).
8. G. Squadrito, O. Barbera, I. Gatto, G. Giacoppo, F. Urbani, E. Passalacqua, CFD analysis of the flow field scale-up influence on the electrodes performance in a PEFC, *Journal of Power Sources*, **Volume 152**, pp.67-74 (2005).
9. *Comsol Multiphysics Advanced Features Course*, Version: December 2005, COMSOL 3.2.